Electronic Supplementary Information (ESI) for Lab on a Chip



# Electronic Supplementary Information

# High-throughput rare cell separation from blood samples using steric hindrance and inertial microfluidics

Shaofei Shen,[a] Chao Ma,[b] Lei Zhao,[b] Yaolei Wang,[a] Jian-Chun Wang,[a] Juan Xu,[a] Tianbao Li,[a] Long Pang[b] and Jinyi Wang*[ab]

[a] *College of Science, Northwest A&F University, Yangling, Shaanxi 712100, China*

[b] *College of Veterinary Medicine, Northwest A&F University, Yangling, Shaanxi 712100, China*

**Abstract.** This supplementary information provides all the additional information as mentioned in the text.

## Materials and reagents

RTV 615 poly(dimethylsiloxane) (PDMS) pre-polymer and curing agent were purchased from Momentive Performance Materials (Waterford, NY, USA); surface-oxidized silicon wafers were from Shanghai Xiangjing Electronic Technology, Ltd. (Shanghai, China); AZ 50XT photoresist and developer were from AZ Electronic Materials (Somerville, NJ, USA); acridine

orange (AO) and propidium iodide (PI) were from Sigma–Aldrich (MO, USA); 15.5-μm diameter polystyrene microspheres fluorescently labeled with dragon green (FS07F) were from Bangs Laboratories, Inc.; and cell culture medium, fetal bovine serum (FBS), and CellTracker Green CMFDA were from Gibco Invitrogen Corporation (CA, USA). The analytical reagent-grade solvents and other chemicals were purchased from local commercial suppliers, unless otherwise stated. All solutions were prepared using ultra-purified water supplied by a Milli-Q system (Millipore®).

**Device fabrication**

The microfluidic devices utilized for this study were fabricated using standard soft lithography with AZ 50XT master mold on a silicon substrate.[1] First, patterns for the microchannels and pillars were designed using AutoCAD software. Second, microchannels and pillars were printed on glass substrates to form a chrome mask (MicroCAD Photomask, Ltd., Suzhou, China). As a result, a mold (57 μm high) was fabricated through a single step under UV light using an AZ 50XT Photoresist on a BG401A mask aligner (7 mW $cm^{-2}$, CETC, China). Before fabricating the microfluidic device, the mold was exposed to trimethylchlorosilane vapor for 2 min to 3 min. A well-mixed PDMS pre-polymer [RTV 615 A and B (10:1, w/w)] was poured onto the mold placed in a Petri dish to yield 3 mm-thick PDMS replica. After degassing, the mold was cured on a hot plate at 80 °C for 50 min. The PDMS replica was then peeled off the mold. Holes for inlets and outlets were punched with a metal pin. Afterward, the PDMS replica was trimmed, cleaned, and placed on a clean glass slide (3000 rpm, 60 s, ramp 15 s) with a PDMS pre-polymer [RTV 615 A and B (20:1, w/w)] cured for 20 min in an oven at 80 °C. Finally, the microfluidic device was ready for use after baking at 80 °C for 48 h.

**Sample preparation**

Isolation of 15.5 μm fluorescent polystyrene microspheres was first performed to primarily explore the separation effect and observe the movement trajectory of the isolates in the designed microfluidic device. The 15.5 μm fluorescent polystyrene microspheres were selected because their size was similar to cancer cell size, and they can be easily observed under a fluorescent microscope. The suspension of the fluorescent microspheres (ρ

~1.06 g/mL) was prepared by diluting the microspheres in ultra-purified water containing 0.5% w/v Tween 20. Prior to each experiment, the microsphere suspension in a 15 mL vial was sonicated for at least 8 min to achieve a sufficiently mono-dispersed suspension.[2]

Three different types of human cancer cell lines, namely, human myelogenous leukemia (K562), human cervical carcinoma (HeLa), and human breast adenocarcinoma (MCF-7), were used to mimic different rare cell separation and enrichment processes for the investigation of rare cell separation. All the cells were obtained from the Chinese Academy of Sciences (Shanghai, China). K562 and HeLa cells were routinely cultured using Dulbecco's modified Eagle's medium (DMEM, Invitrogen, Grand Island, NY) supplemented with 10% FBS (Invitrogen), 100 U/mL penicillin, and 100 μg/mL streptomycin. MCF-7 cells were routinely cultured with Roswell Park Memorial Institute medium 1640 (RPMI-1640 medium, Invitrogen, Grand Island, NY) supplemented with 10% FBS, 100 U/mL penicillin, and 100 μg/mL streptomycin. The cells were then placed in a humidified atmosphere with 5% $CO_2$ at 37 °C. The cells were normally passaged at a ratio of 1:3 every 3 days to maintain their exponential growth phase. HeLa and MCF-7 cells were harvested through trypsinization with 0.25% trypsin (Invitrogen) in $Ca^{2+}$ and $Mg^{2+}$ free Hanks' balanced salt solution at 37 °C before use. Trypsinization was stopped upon the addition of fresh supplemented culture medium, and then the cell suspension was centrifuged at a rotational speed of 800 rpm for 3 min. Given that K562 cells are rounded, nonadherent, and grow in suspension, the cells were harvested directly after centrifugation at 1000 rpm for 3 min.

The rare cell suspensions for their respective isolation study were prepared by suspending K562, HeLa, or MCF-7 cells in PBS working buffer (PBS, 0.01 mol/L, PH 7.4; citric acid, 4.8 g/L; trisodium citrate, 13.2 g/L; and dextrose, 14.7 g/L) supplemented with 1% bovine serum albumin (Invitrogen) to prevent cell sedimentation and non-specific adsorption to the microchannels during separation.[3] For the blood cell tests, whole blood samples were obtained from healthy volunteers and collected into ethylenediaminetetraacetic acid vacuum tubes. Prior to use, the samples were diluted to 1:5, 1:20, 1:40, and 1:80 (v:v) with the above PBS working buffer, corresponding to hematocrits (Hct) of 8%, 2%, 1%, and 0.5%,

respectively. All blood samples were used within 6 h of collection. For rare cell isolation study from the blood samples, the rare cells were first stained with CellTracker Green CMFDA. The harvested K562 cells in the suspension were first centrifuged, and then the supernatant was aspirated. Afterward, the cells were resuspended gently in a pre-warmed CellTracker Green CMFDA solution to stain for 30 min in a humidified atmosphere with 5% $CO_2$ at 37 °C. Then, staining of HeLa and MCF-7 cells was performed. The culture medium was removed when the cells reached the exponential growth phase, after which pre-warmed CellTracker Green CMFDA solution was added to stain the cells for 30 min in a humidified atmosphere with 5% $CO_2$ at 37 °C. The cells were stained to facilitate observation of rare cell and counting of cells that recovered. The stained cells were centrifuged, diluted with PBS working buffer, and then resuspended in healthy human blood for further use.

After evaluating the isolation effect of the designed microfluidic device using microspheres ($10^4$ /mL), each type of rare cell line suspension ($10^2$, $10^3$, and $10^4$ cells/mL), and the actual blood samples with various Hct (8%, 2%, 1%, and 0.5%), each fluorescence-labeled rare cell line ($10^2$, $10^3$, and $10^4$ cells/mL) was spiked into unstained 40× diluted whole blood ($1.32\times10^8$ cells/mL) to model the low events of rare cells in blood and then applied for isolation study of rare cells from the blood samples. Specifically, the spiked HeLa cell suspension included single cells and 4 to 10 irregular gathering cells to mimic the CTC clusters because clustered cells yield important prognostic significance in clinical samples.[4] All concentrations of the cells were determined using hemocytometer method.[5]

**Numerical simulations**

To evaluate velocity field fluctuations in the device, computational fluid dynamics (CFD) simulation was performed using ESI-CFD software (V2010.0, ESI CFD, Inc.). The simulation environment was verified for steady incompressible flows. Different Reynolds number flows ($Re_c$) were specified at the input, and the outlet was set to a fixed-pressure boundary condition. No slip boundary condition was applied at the channel walls. FLOW and TURBULENCE modules in CFD-ACE+ were used to explore the flow velocity distribution in the microchannels. Based on the finite volume method, the conservation of Navier–Stokes

momentum in the device is described by Equation (1) as follows:

$$\frac{\partial}{\partial t}\left(\rho\vec{V}\right)+\nabla\bullet\left(\rho\vec{V}\vec{V}\right)=-\nabla P+\nabla\bullet\bar{\bar{\tau}} \quad (1)$$

The conservation of mass is described by the continuity Equation (2) as follows:

$$\frac{\partial\rho}{\partial t}+\nabla\bullet\left(\rho\vec{V}\right)=0 \quad (2)$$

The local turbulent Reynolds number ($Re_t$) is expressed as follows:

$$Re_t=\frac{k^2}{v\varepsilon} \quad (3)$$

where $\rho$ is fluid density; $\vec{V}$ is velocity vector; $P$ is pressure; $\bar{\bar{\tau}}$ is stress tensor; $k$ is turbulent kinetic energy; $\varepsilon$ is rate of dissipation, and $v$ is turbulent viscosity.

**Isolation efficiency**

The collection and enrichment efficiency of cancer cells were calculated using the following equations:

$$\text{Collection efficiency} = \frac{n_{outlet\,1}R_{outlet\,1}}{n_{inlet}R_{inlet}}\times 100\% \quad (4)$$

$$\text{Enrichment efficiency} = \frac{R_{outlet\,1}}{R_{inlet}} \quad (5)$$

$$\text{Purity} = \frac{n_{outlet\,1}R_{outlet\,1}}{n_{outlet\,1}R_{outlet\,1}+n_{outlet\,1}}\times 100\% \quad (6)$$

Where $n_{outlet\,1}$ is the number density of blood cells, collected from the outlet 1, $n_{inlet}$ is that in the original sample, $R_{outlet\,1}$ is the ratio of cancer cells to blood cells in a sample collected from the outlet 1, $R_{inlet}$ is that in the original sample.

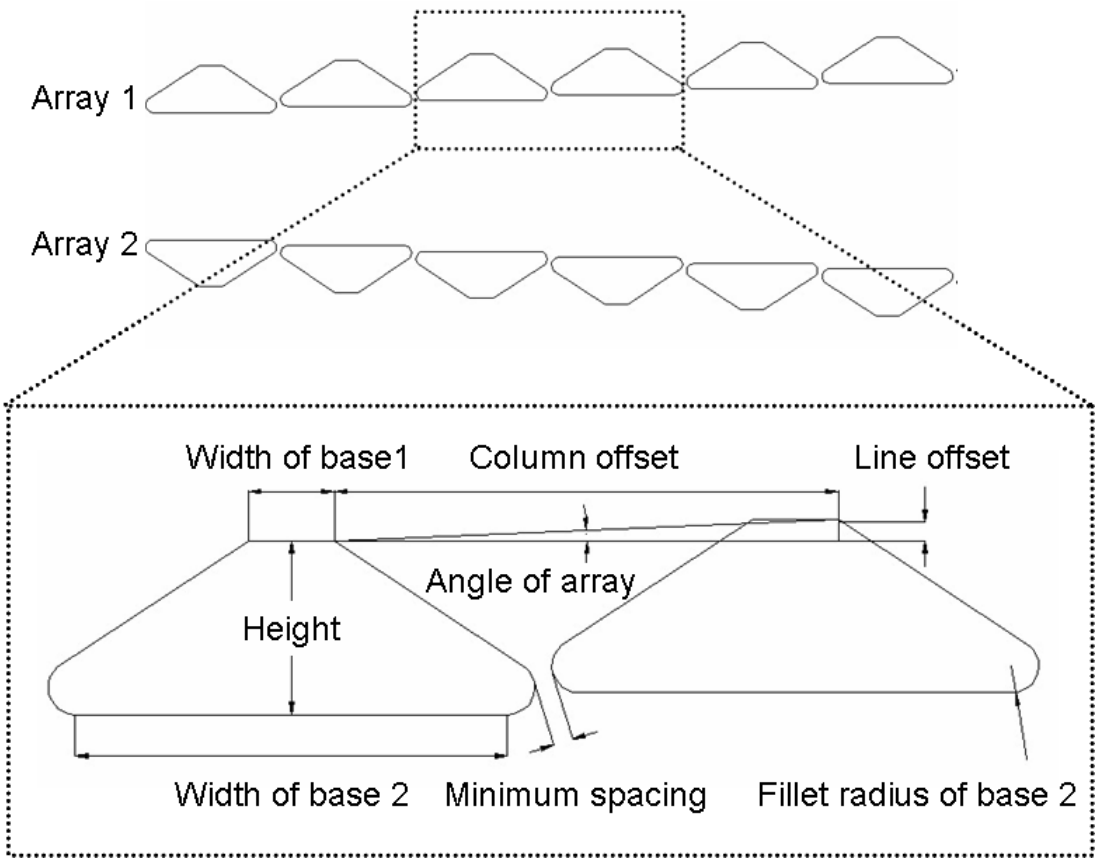


**Fig. S1.** Schematic diagram of the steric hindrance region in the microfluidic device. The amplifying image shows the design diagram of array 1 (more detailed design parameters can be found in Table S1).

**Table S1.** Detailed design parameters of the devices used in the current study.

| Parameters | Device Number | | |
|---|---|---|---|
| | Device 1 | Device 2 | Device 3 |
| Width of base 1 (μm) | 40 | 40 | 40 |
| Width of base 2 (μm) | 200 | 200 | 200 |
| Height (μm) | 80 | 80 | 80 |
| Fillet radius of base 2 (μm) | 10 | 10 | 10 |
| Line offset (μm) | 5 | 10 | 15 |
| Column offset (μm) | 233.94 | 232.90 | 231.30 |
| Angle of array 1 (◦) | 1 | 2 | 4 |
| Angle of array 2 (◦) | - 1 | - 2 | - 4 |
| | 10 | 10 | 10 |

| | | | |
|---|---|---|---|
| Minimum spacing (μm) | 31 | 16 | 11 |
| Number of arrays | | | |

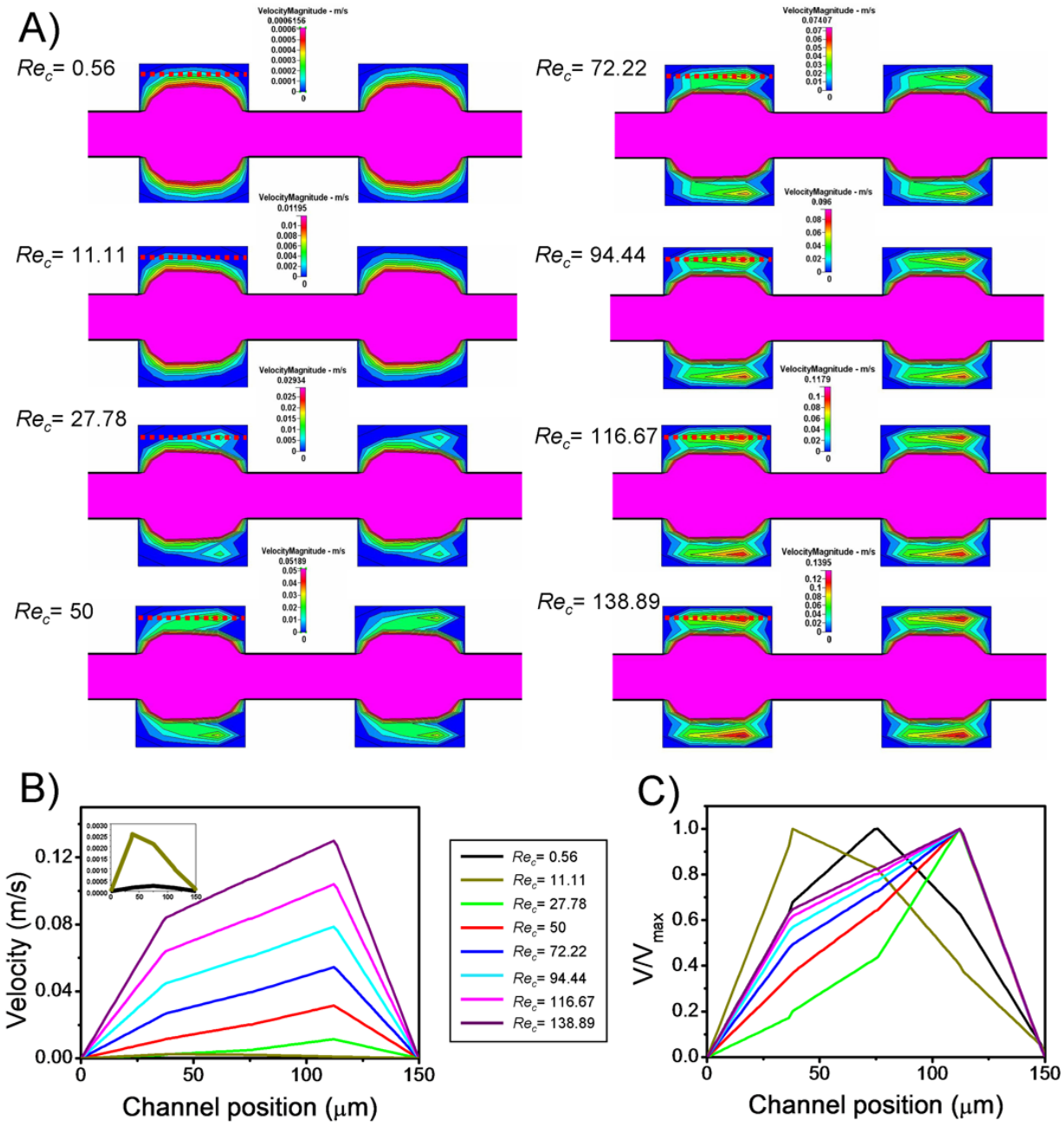


**Fig. S2.** Computational simulation of the fluid velocities in the inertial focusing region under various channel Reynolds numbers ($Re_c$). (A) Various fluid velocity patterns were formed in the inertial focusing region under various $Re_c$. The width of contraction channel is 60 μm. The red dotted lines were used to analyze fluid velocity distributions at the same lateral positions. Quantitative comparison of fluid velocities (B) and ratios (C) of the flow velocity to the maximum flow velocity ($v/v_{max}$) under various $Re_c$ at the same lateral positions which

correspond to the positions of red dotted lines in (A).

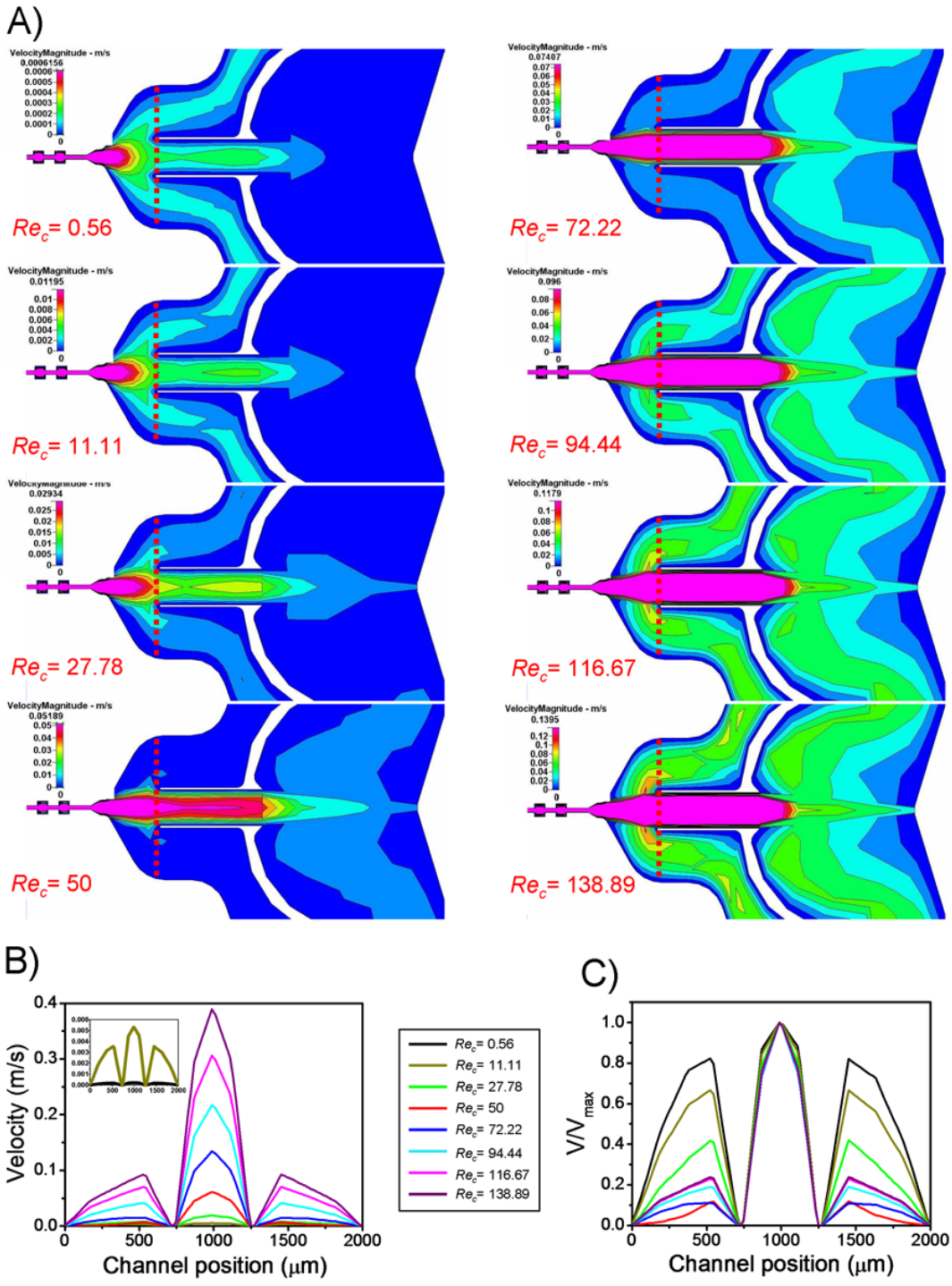


**Fig. S3.** Computational simulation of the fluid velocities in the inertial separation region under various $Re_c$. (A) Various fluid velocity patterns were formed in the inertial separation region under various $Re_c$. The red dotted lines were used to analyze fluid velocity distributions at the

same longitudinal positions. Comparison of fluid velocities (B) and ratios (C) of the flow velocity to the maximum flow velocity ($v/v_{max}$) under various $Re_c$ at the same longitudinal positions which correspond to the positions of red dotted lines in (A).

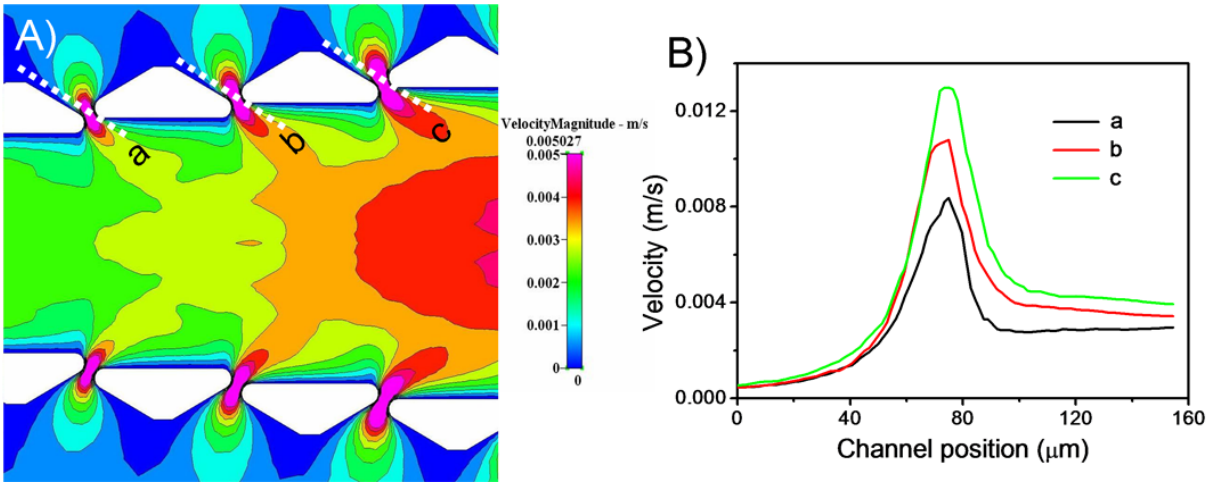


**Fig. S4.** Computational simulation of the fluid velocities in the steric hindrance region under $Re_c$ = 72.22. (A) Fluid velocity pattern was formed in the steric hindrance region under $Re_c$ = 72.22. The white dotted lines were used to analyze the fluid velocity distributions between the isosceles trapezoid-shaped pillars. (B) Quantitative comparison of fluid velocities under $Re_c$ = 72.22 between different isosceles trapezoid-shaped pillars, which correspond to the positions of white dotted lines in (A).

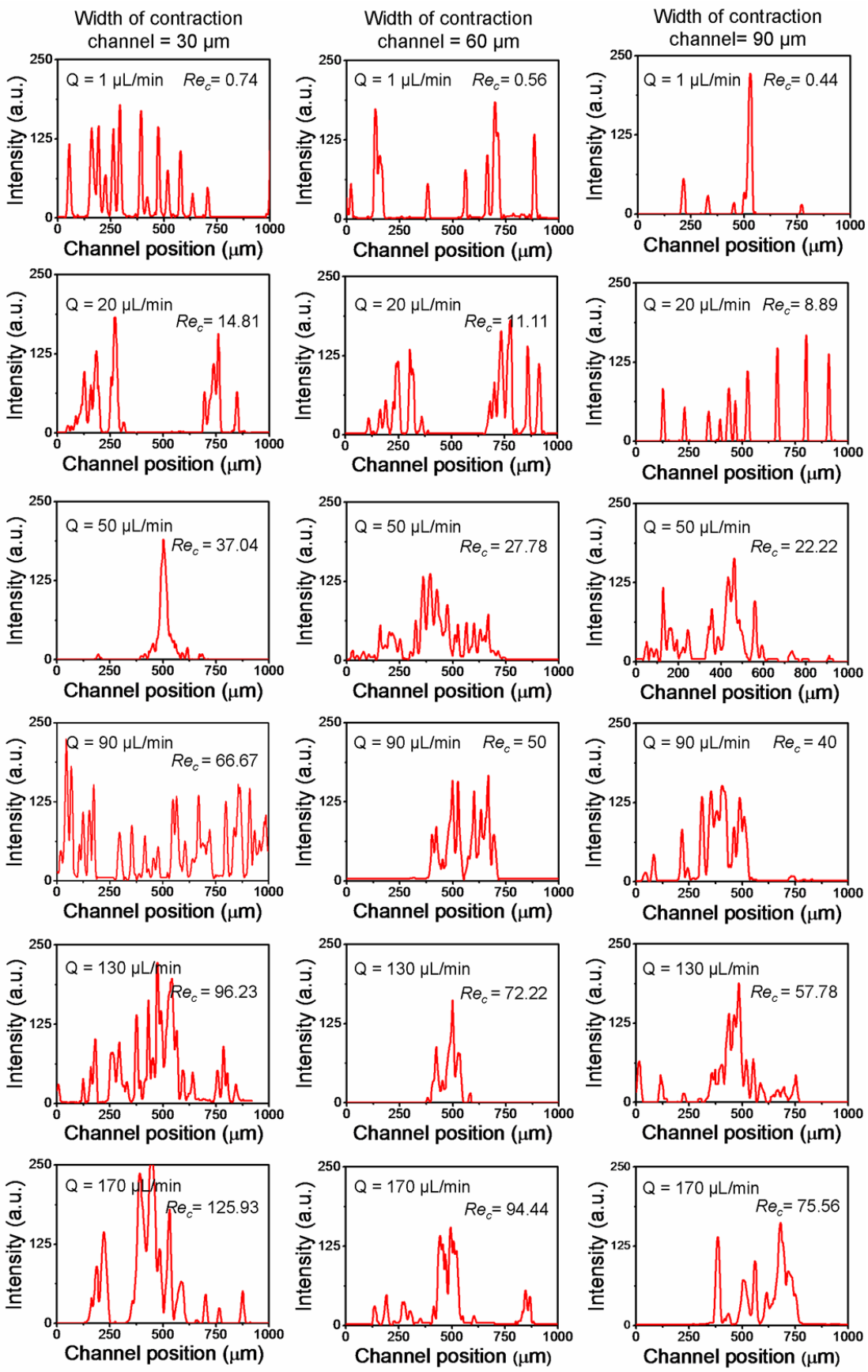


**Fig. S5.** Fluorescence intensity analysis of the fluorescence microspheres under various $Re_c$ in the inertial separation region, which correspond to the red dotted lines in Fig. 2.

**Table S2.** Collection efficiency of fluorescence microspheres under various $Re_c$ in the inertial separation region after passing through three different widths of contraction channels (30, 60, and 90 μm) of the inertial focusing region.

| Q (μL/min) | | 1 | | | 20 | | | 50 | | | 90 | | | 130 | | | 170 | | |
|---|---|---|---|---|---|---|---|---|---|---|---|---|---|---|---|---|---|---|---|
| Channels (μm) | | 30 | 60 | 90 | 30 | 60 | 90 | 30 | 60 | 90 | 30 | 60 | 90 | 30 | 60 | 90 | 30 | 60 | 90 |
| $Re_c$ | | 0.74 | 0.56 | 0.44 | 14.81 | 11.11 | 8.89 | 37.04 | 27.78 | 22.22 | 66.67 | 50 | 40 | 96.23 | 72.22 | 57.78 | 125.93 | 94.44 | 75.56 |
| $Re_p$ | | 0.10 | 0.03 | 0.02 | 2.08 | 0.69 | 0.39 | 5.21 | 1.74 | 0.97 | 9.38 | 3.13 | 1.74 | 13.54 | 4.51 | 2.51 | 17.71 | 5.90 | 3.28 |
| Recovery | Center | 41.27 | 56.82 | 85.74 | 36 | 42.44 | 58.33 | 98.93 | 65.44 | 59.35 | 43.58 | 90.91 | 68.77 | 60.61 | 99.42 | 80.54 | 76.34 | 85.69 | 88.32 |
| | Side | 58.73 | 43.18 | 14.26 | 64 | 57.56 | 41.67 | 1.07 | 34.56 | 40.65 | 56.42 | 9.09 | 31.23 | 39.39 | 0.58 | 19.46 | 23.66 | 14.31 | 11.68 |

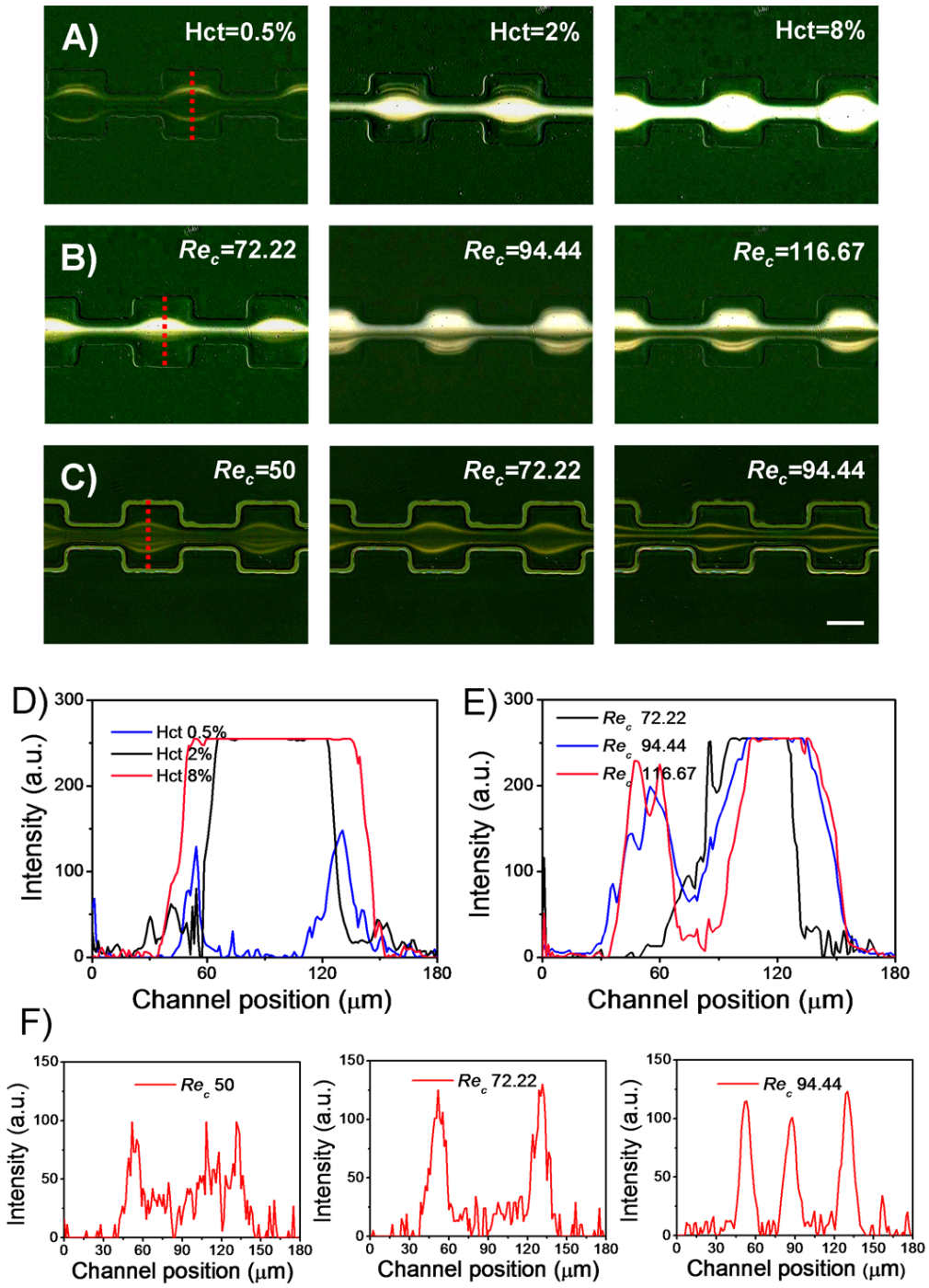


**Fig. S6**. Effects of Hct and $Re_c$ on blood cell trajectories in the inertial focusing region (width of contraction channel = 60 μm). Images illustrate blood cell trajectories for increasing Hct (A, Hct from 0.5% to 8%, $Re_c$ = 72.22), $Re_c$ (B, $Re_c$ from 72.22 to 116.67, Hct = 2%), and $Re_c$ (C, $Re_c$ from 50 to 94.44, Hct = 1%). The red dotted lines were used to analyze blood cell distributions at the same longitudinal positions. Analytical results are listed in D, corresponding to A; E, corresponding to B; and F, corresponding to C, respectively. Scale bar, 100 μm.

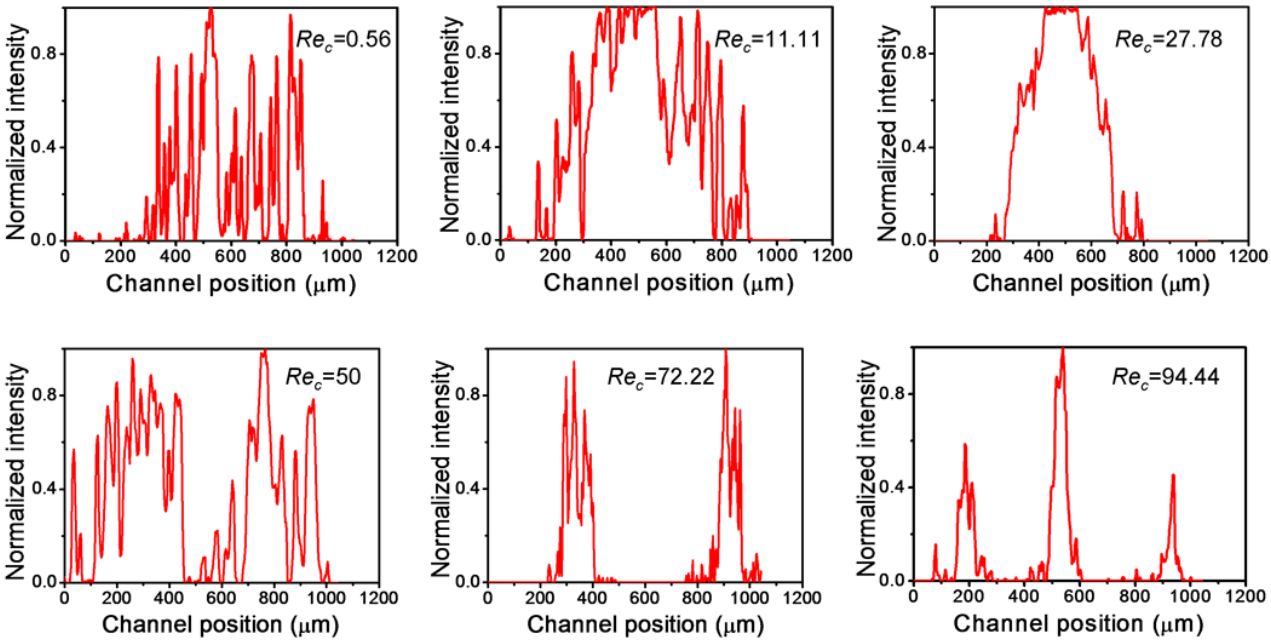


**Fig. S7.** Normalized light intensity indicating blood cell trajectories under various $Re_c$ in the inertial separation region, corresponding to the red dotted lines in Fig. 3(A).

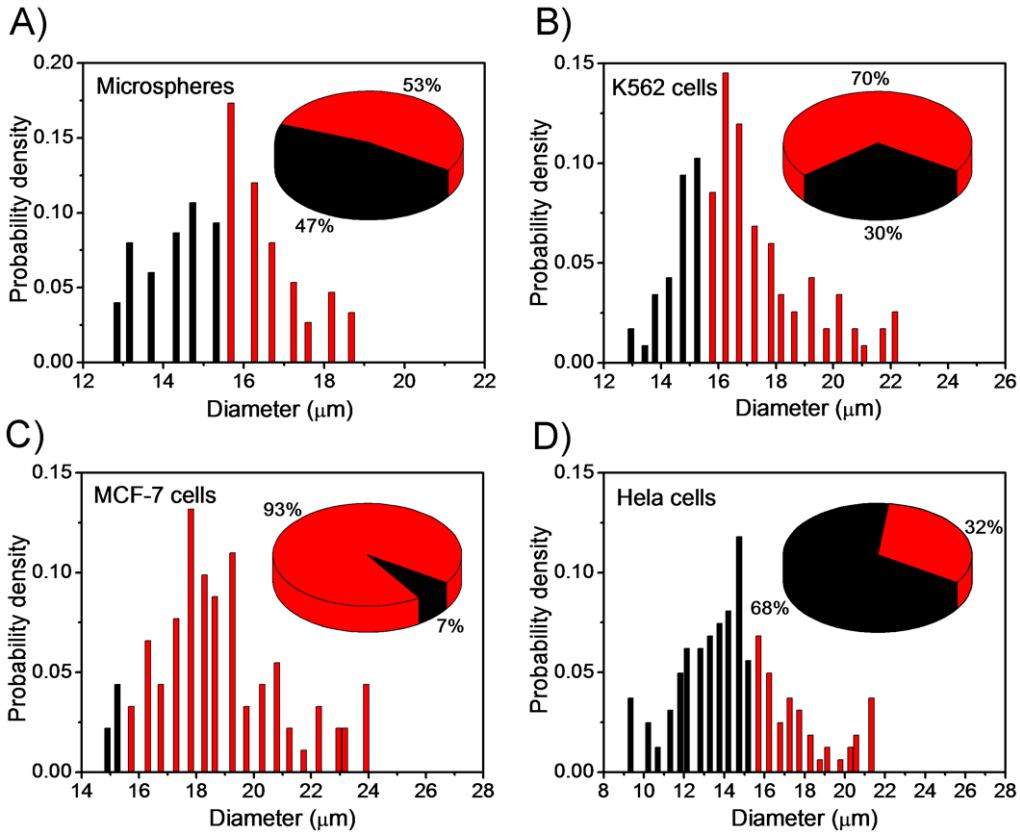


**Fig. S8.** Probability density distribution of the microsphere and rare cell (K562, MCF-7, and HeLa cells) diameters. Pie chart insets illustrate the proportion of microspheres/cells with diameters below and above the cutoff size of $\alpha_{cutoff}$ ~ 15.5 μm.

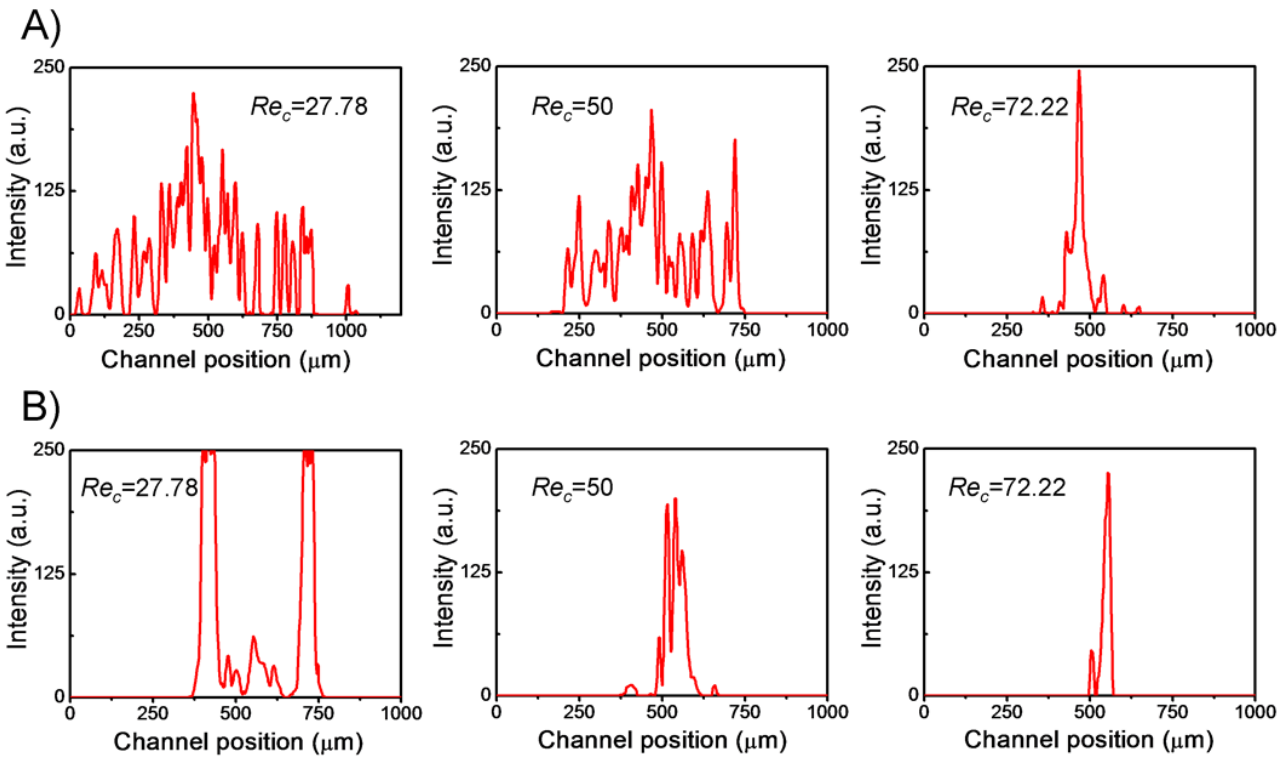


**Fig. S9.** Fluorescence intensity analysis indicating the microsphere trajectories under various $Re_c$ in the steric hindrance region. (A) and (B) correspond to the red dotted lines in Figs. 4(A) and (B), respectively.

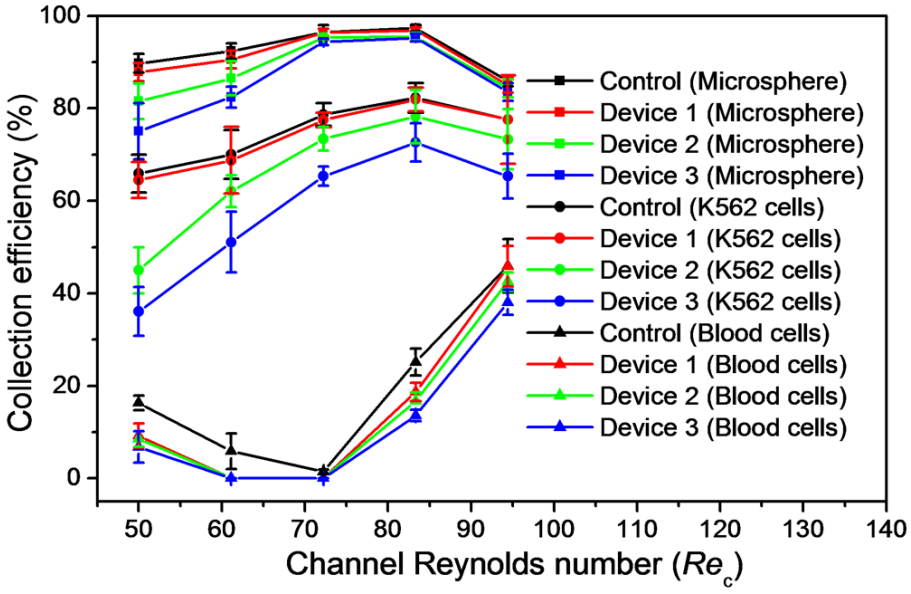


**Fig. S10.** Plots presenting the effects of μITPAR on the collection efficiency of microspheres ($10^4$ cells/mL), K562 cells ($10^4$ cells/mL), and blood cells (1% Hct) with increasing $Re_c$, respectively. Control groups represent the sample collection efficiency without steric hindrance region.

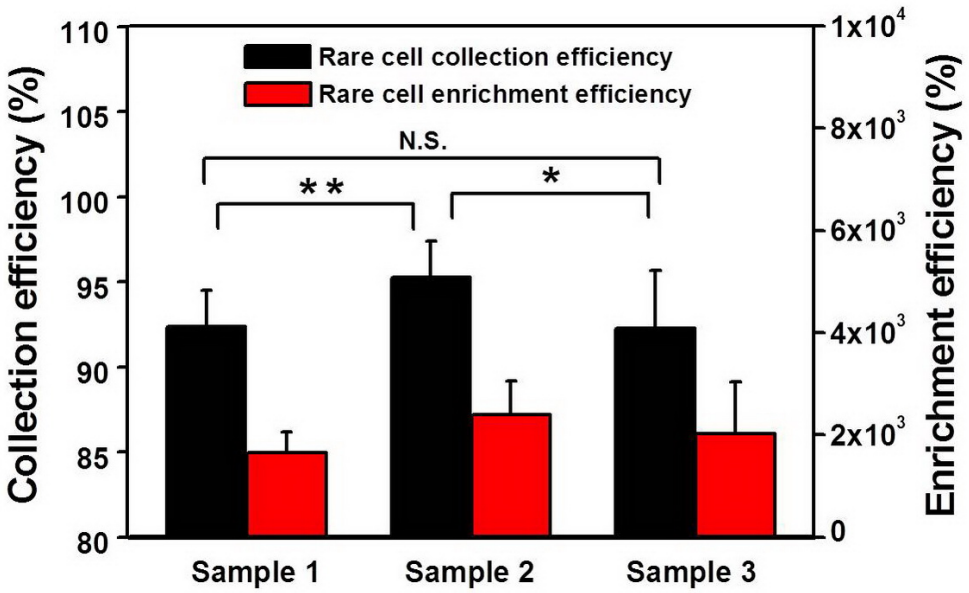


**Fig. S11.** Evaluation of microfluidic system performance without steric hindrance region using rare cells (K562, MCF-7, and HeLa cells). Statistical results of collection efficiency and enrichment efficiency of rare cells at rare cell-to-blood cell ratio of $1/10^6$. Each type of independent rare cell spiked into diluted whole blood (sample 1, K562 cells; sample 2, MCF-7 cells; and sample 3, HeLa cells) was tested using optimum test conditions (1% Hct blood and $Re_c$ = 72.22). Standard deviations deduced from ten parallel experiments are shown as the error bars, with the significance assessed by ANOVA. $^{**}P < 0.01$; $^{*}P < 0.05$; N.S., not significant.

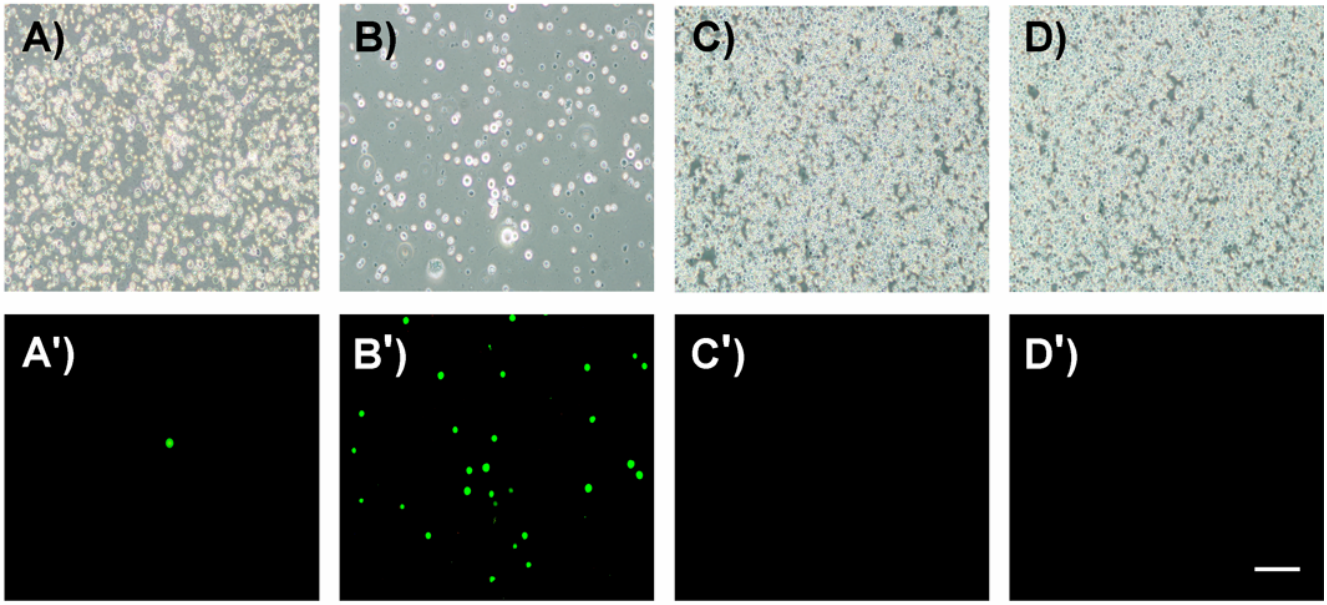


**Fig. S12.** Comparison of bright-field (A–D) and fluorescence (A' to D') images of the mixture of K562 and blood cells before separation (A and A'), cells collected from outlet 1 (B and B'), cells from outlet 2 (C and C'), and cells from outlet 3 (D and D'). In the study, the ratio of K562 cells-to-blood cells is $1/10^6$ and $Re_c$ = 72.22. In addition, to facilitate the count of cell recovery, K562 cells were stained with CellTracker Green. The results show that the rare cells K562 were well enriched with a purity of 13.1%. Scale bar, 200 μm.

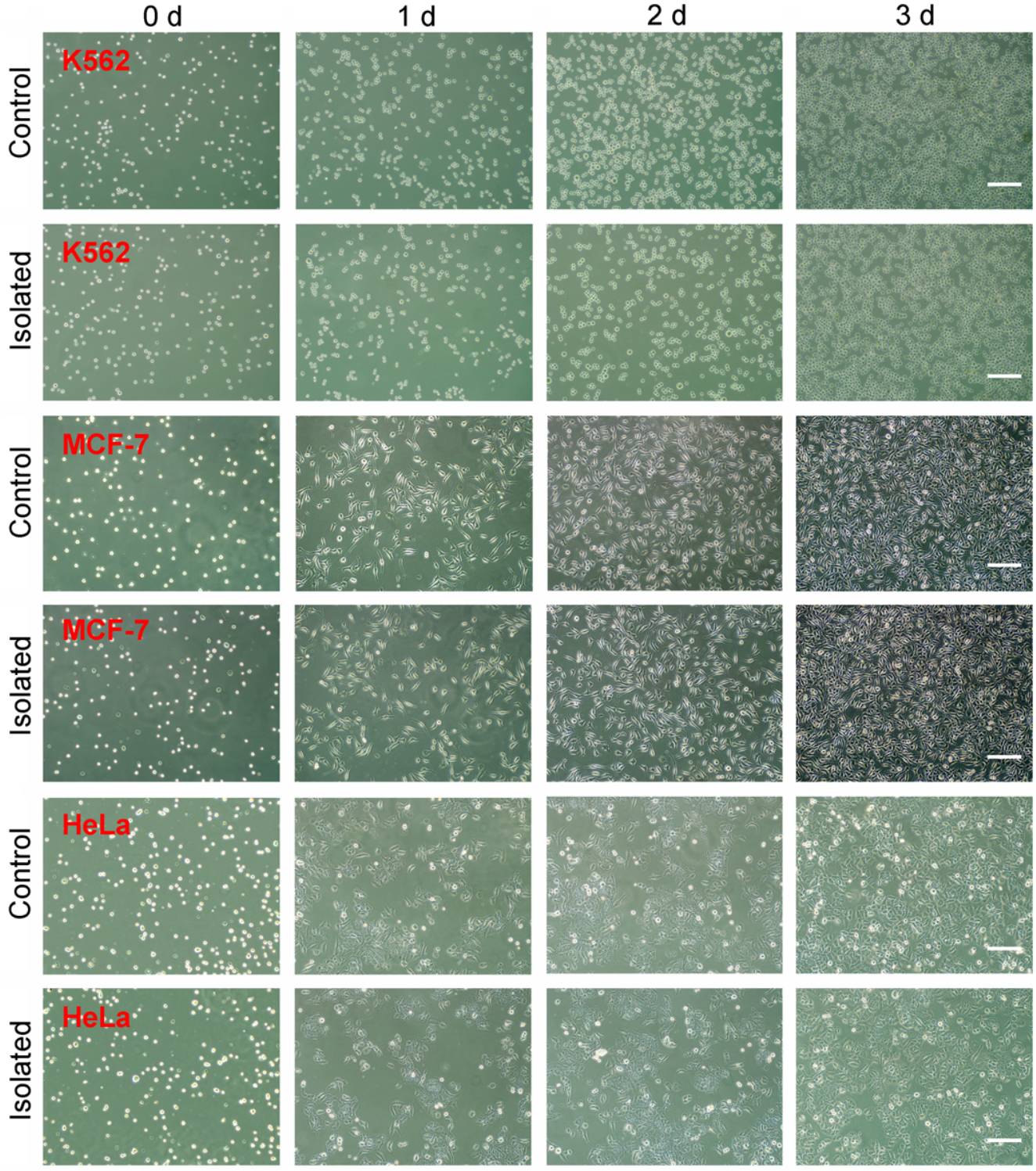


**Fig. S13.** Rare cell (K562, MCF-7, and HeLa cells) viability assay by reseeding them back into culture. The bright-field images of cultures of control (unseparated) and separated rare cells ($10^4$ cells/mL) collected from outlet 1 of the microfluidic device at $Re_c$ = 72.22. The images indicate no significant differences between morphology and proliferation rate of the rare cells, suggesting high viability and integrity. Scale bars, 200 μm.

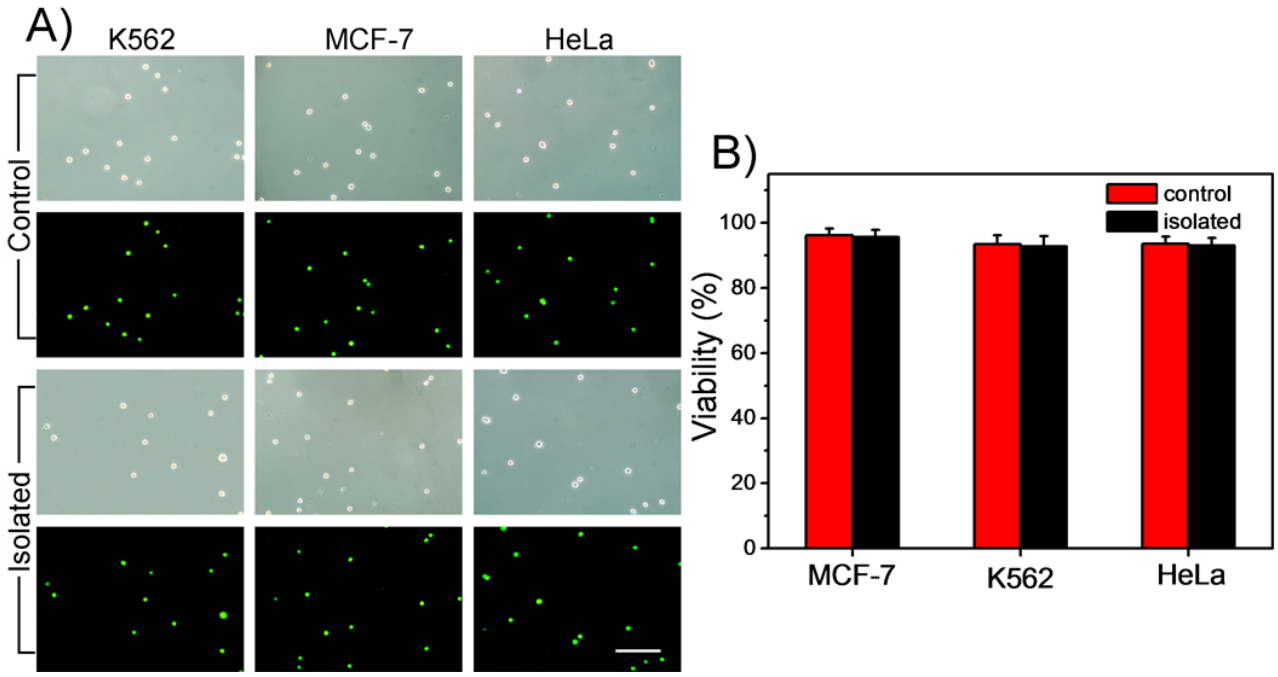


**Fig. S14.** Comparison of cell viability between control (unseparated) and separated rare cells (K562, MCF-7, and HeLa cells) using AO/PI double-staining method. (A) The bright-field (top) and fluorescence (bottom) images of control (rows 1 and 2) and separated (rows 3 and 4) rare cells. (B) Quantitative analysis of cellular viability of control (unseparated) and separated rare cells. The results confirm that cells separated through the microfluidic system remain highly viable, similar to control cells, retrieving > 92% viable cells. Scale bars, 100 μm.

## References

1 J. Sha, Y. Wang, J. C. Wang, W. Liu, Q. Tu, A. Liu, L. Wang and J. Wang, *Anal. Methods*, 2011, **3**, 1988–1994.

2 J.-S. Park, S.-H. Song and H.-I. Jung, *Lab Chip*, 2009, **9**, 939–948.

3 A. A. S. Bhagat, H. W. Hou, L. D. Li, C. T. Lim and J. Han, *Lab Chip*, 2011, **11**, 1870–1878.

4 S. L. Stott, C.-H. Hsu, D. I. Tsukrov, M. Yu, D. T. Miyamoto, B. A. Waltman, S. M. Rothenberg, A. M. Shah, M. E. Smas, G. K. Korir, F. P. Floyd, A. J. Gilman, J. B. Lord, D. Winokur, S. Springer, D. Irimia, S. Nagrath, L. V Sequist, R. J. Lee, K. J. Isselbacher, S. Maheswaran, D. A. Haber and M. Toner, *Proc. Natl. Acad. Sci. U. S. A.*, 2010, **107**, 18392–18397.

5 J. Sun, M. Li, C. Liu, Y. Zhang, D. Liu, W. Liu, G. Hu and X. Jiang, *Lab Chip*, 2012, **12**, 3952–3960.

**ESI Movies**

**Movie S1.** Trajectories of fluorescence microspheres in the inertial separation region. Time-lapse fluorescence images were acquired continuously when microspheres formed a single band in the centerline of the inertial separation region at $Re_c$ = 72.22.

**Movie S2.** Trajectories of blood cells in the inertial focusing region and inertial separation region. Time-lapse optical images were acquired continuously while three-band blood cell (1% Hct) distributions occurred at $Re_c$ = 94.44.

**Movie S3.** Trajectories of K562 cells (spiked in diluted whole blood) in the inertial separation region. Time-lapse optical images were acquired continuously, showing separation of K562 cells ($10^2$/mL, spiked in 1% Hct blood) at $Re_c$ = 72.22. The large K562 cells and a few blood cells passed through the center channel, whereas most blood cells exited through the two side channels.

**Movie S4.** Trajectories of fluorescence microspheres in the steric hindrance region. Time-lapse fluorescence images were acquired continuously while microspheres formed a single band in the centerline of the steric hindrance region at $Re_c$ = 72.22.

**Movie S5.** Trajectories of K562 cells (in PBS working buffer) in the steric hindrance region. Time-lapse optical images were acquired continuously, showing trajectories of K562 cells ($10^4$/mL) at $Re_c$ = 72.22. The K562 cells could not form a single band in the centerline of the steric hindrance region, but they could be transported by μITPAR into outlet 1.